

I am pleased to provide you complimentary one-time access to my article as a PDF file for your own personal use. Any further/multiple distribution, publication or commercial usage of this copyrighted material would require submission of a permission request to the publisher.

Timothy M. Miller, MD, PhD

Increased 4R-Tau Induces Pathological Changes in a Human-Tau Mouse Model

Highlights

- Antisense oligonucleotide-mediated *MAPT* splicing is successful in vivo
- Increasing 4R-tau induces tau phosphorylation and exacerbates seizures
- Reducing 4R-tau is effective in human tau-expressing mouse models

Authors

Kathleen M. Schoch, Sarah L. DeVos, Rebecca L. Miller, ..., C. Frank Bennett, Frank Rigo, Timothy M. Miller

Correspondence

millert@neuro.wustl.edu

In Brief

Schoch et al. employ antisense oligonucleotide technology to manipulate tau isoforms, demonstrating that increased four-repeat tau drives toxic changes in a human tau mouse model. Reducing four-repeat tau was also achieved, suggesting application in human tauopathies.

Increased 4R-Tau Induces Pathological Changes in a Human-Tau Mouse Model

Kathleen M. Schoch,^{1,5} Sarah L. DeVos,^{1,5} Rebecca L. Miller,¹ Seung J. Chun,² Michaela Norrbom,² David F. Wozniak,³ Hana N. Dawson,⁴ C. Frank Bennett,² Frank Rigo,² and Timothy M. Miller^{1,*}

¹Department of Neurology, Hope Center for Neurological Disorders, Washington University in St. Louis, St. Louis, MO 63110

²Ionis Pharmaceuticals, Carlsbad, CA 92010

³Taylor Family Institute for Innovative Psychiatric Research, Department of Psychiatry, Washington University in St. Louis, St. Louis, MO 63110

⁴Department of Neurology, Duke University Medical Center, Durham, NC 27710

⁵Co-first author

*Correspondence: millert@neuro.wustl.edu

<http://dx.doi.org/10.1016/j.neuron.2016.04.042>

SUMMARY

Pathological evidence for selective four-repeat (4R) tau deposition in certain dementias and exon 10-positioned *MAPT* mutations together suggest a 4R-specific role in causing disease. However, direct assessments of 4R toxicity have not yet been accomplished in vivo. Increasing 4R-tau expression without change to total tau in human tau-expressing mice induced more severe seizures and nesting behavior abnormality, increased tau phosphorylation, and produced a shift toward oligomeric tau. Exon 10 skipping could also be accomplished in vivo, providing support for a 4R-tau targeted approach to target 4R-tau toxicity and, in cases of primary *MAPT* mutation, eliminate the disease-causing mutation.

INTRODUCTION

Cognitive disorders including Alzheimer's disease (AD) and primary tauopathies are typified by the abnormal intracellular deposition of the microtubule-associated protein tau. Tau can be expressed with three-repeat (3R) or four-repeat (4R) domains, which arise from alternative splicing of *MAPT* exon 10 mRNA. Normal adult humans express approximately equal 3R-tau and 4R-tau; however, select sporadic tauopathies exhibit an imbalance of 4R-tau isoform deposition within neurofibrillary tangles (NFTs) (Arai et al., 2001; de Silva et al., 2003). In patients with frontotemporal dementia with parkinsonism linked to chromosome 17 (FTDP-17), mutations identified within *MAPT* exon/intron 10 result in an abnormal increase in 4R-tau expression without disruption of its microtubule binding characteristics (D'Souza et al., 1999; Hong et al., 1998).

While some in vitro studies demonstrate that 4R-tau or an altered isoform ratio induces tau aggregation (Adams et al., 2010; von Bergen et al., 2001), testing 3R-tau versus 4R-tau toxicity in animal models has been challenging because mice do not recapitulate human 4R:3R ratios, and different transgenes

are not directly comparable. We developed tau isoform switching antisense oligonucleotides (ASOs) (DeVos and Miller, 2013a) for use in hTau mice, which lack endogenous mouse tau and express mostly 3R human tau (Andorfer et al., 2003) without early onset behavioral deficits or tau pathology (Polydoro et al., 2009). By comparing mice of the same genetic background but greater ASO-driven 4R-tau, we were able to test whether increased 4R-tau led to increased pathology and changes in behavior. In addition, we demonstrate the feasibility of a 4R-reducing therapeutic approach using ASOs.

RESULTS

Characterization of 3R to 4R ASO Treatment in hTau Mice

In order to test whether 4R-tau is a prime mediator of tauopathy, we developed ASOs that target human *MAPT* mRNA to increase the 4R:3R tau ratio. hTau mice were treated with continuous intraventricular infusion of saline, scrambled ASO, or 3R to 4R *MAPT* mRNA splicing ASO for 28 days via osmotic pump. One month following cessation of infusion, mRNA analysis revealed a nearly 2-fold increase in 4R human *MAPT* mRNA with splicing ASO treatment (n = 19) compared to saline-treated or scrambled ASO-treated mice (n = 9/group; p < 0.005 versus saline and scrambled controls, Figure 1A). Importantly, there was no alteration of total human tau (Figures 1B and 1C), indicative of an isoform switch rather than a 4R-tau increase alone. ASO-mediated *MAPT* alteration also occurred in the absence of off-target binding (see Figure S1 available online). 4R, 3R, and total tau protein expression closely corresponded to *MAPT* mRNA levels, revealing an increase in 4R-tau and decrease in 3R-tau following 3R to 4R splicing treatment (Figure 1D) with similar total tau levels (Figures 1E and 1F).

3R to 4R *MAPT* mRNA Splicing in hTau Mice Modifies Tau Phosphorylation, Aggregation, and Solubility

3R to 4R splicing ASO-treated hTau mice were evaluated for tau phosphorylation using the AT8 antibody, which detects S202/T205 phosphorylation events and is frequently associated with tau pathology (Braak and Braak, 1995). Following scrambled ASO treatment (n = 5), faint neuronal AT8 immunoreactivity

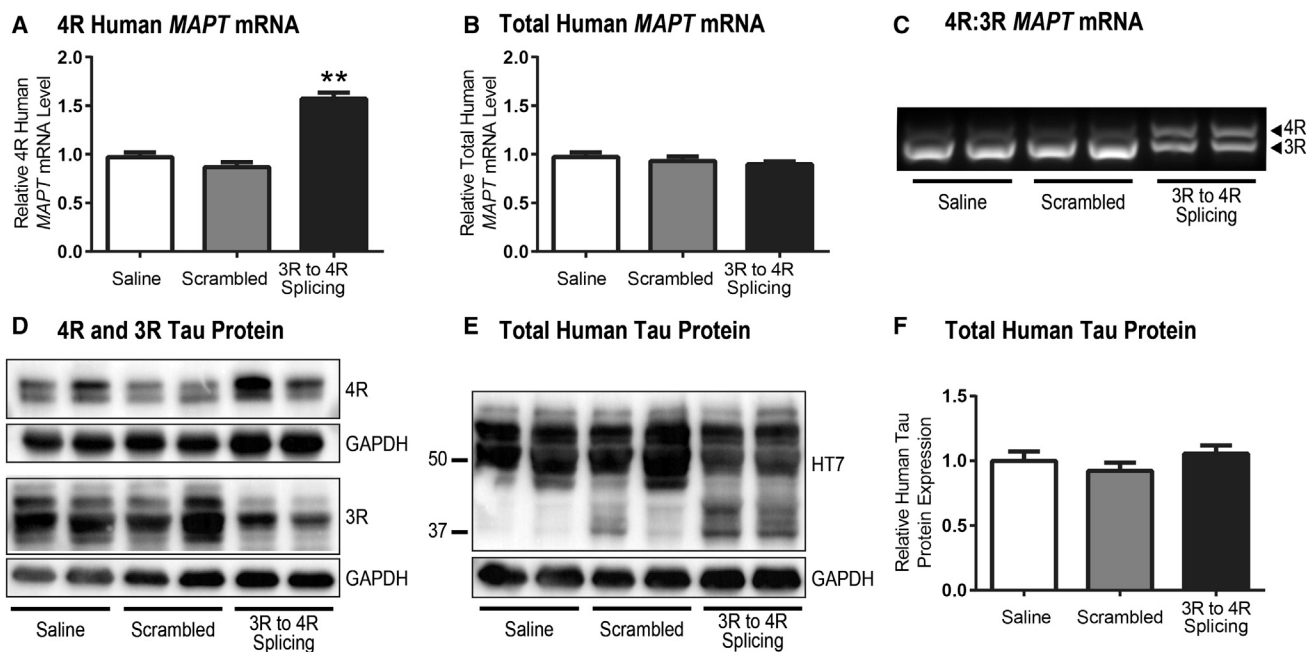


Figure 1. Total Tau and Tau Isoform mRNA and Protein Expression in hTau Mice following 3R to 4R MAPT mRNA Splicing ASO Treatment (A and B) (A) Relative 4R human MAPT mRNA was significantly increased following 3R to 4R splicing ASO administration, while (B) total MAPT mRNA levels remained similar to controls (n = 19 splicing ASO, n = 9/saline and scrambled controls). MAPT mRNA data were normalized to GAPDH and the mean + SEM calculated relative to saline controls; **p < 0.005 compared to saline and scrambled control values. (C) 3R and 4R MAPT mRNA products visualized following RT-PCR confirm a shift in isoform composition following 3R to 4R splicing ASO treatment compared to mice treated with saline or scrambled ASO. (D and E) (D) Immunoblots for 3R-tau and 4R-tau show greater 3R-tau protein compared to 4R-tau in brain homogenates obtained from saline- and scrambled-treated mice, ipsilateral to the catheter placement. With 3R to 4R splicing ASO administration, the ratio of tau isoforms is altered, increasing the expression of 4R-tau and decreasing expression of 3R, (E) without changing total tau protein (HT7). (F) Total human tau protein expression quantified by human tau-specific ELISA closely paralleled total MAPT mRNA results, showing no change in total human tau protein after treatment. Data are expressed as mean + SEM relative to saline controls.

was identified within the entorhinal cortex (Figure 2A) and amygdala (Figure 2D) and throughout the cortex (Figure 2G). However, with 3R to 4R splicing ASO treatment (n = 7), the area of positive immunoreactivity increased (Figures 2B, 2E, and 2H), showing significantly higher percentages of staining within select areas (p < 0.05; Figures 2C, 2F, and 2I). Exacerbated AT8 reactivity within known regions of tau spread throughout the brain may be predictive of increased pathological tau burden with greater 4R-tau expression.

Tau aggregation into larger, more insoluble species is also a characteristic of fibrillar structures and increasing toxicity (Spillantini and Goedert, 2013). Therefore, cortical brain tissue from 12-month-old hTau mice treated with scrambled ASO (n = 3) or 3R to 4R splicing ASO (n = 4) was analyzed for high-molecular-weight (HMW) tau forms. Greater tau reactivity was evident within HMW regions with 3R to 4R splicing ASO treatment compared to controls (Figure 2J). Not only was this result indicative of aggregated tau proteins with increased 4R-tau, but also regions of HMW tau were determined to be more heavily phosphorylated (p < 0.05; Figure 2K; Figure S2). To further confirm 4R-tau-driven pathology, soluble and insoluble tau species were identified by fractionation analysis of cortical brain tissue from treated hTau mice. While the majority of tau within hTau mice was found within the RAB-soluble fraction, increased 4R-

tau was associated with a moderate increase RIPA-soluble tau, indicating a decline in solubility (Figure 2L). Insoluble tau detected within the formic acid fraction did not change. Human-tau-specific ELISA analysis mirrored the increase in RIPA-soluble tau (Figure 2M). Both SDD-AGE and fractionation results are consistent with phosphorylated tau histology, collectively suggesting human tau is becoming more phosphorylated, aggregated, and less soluble with increased 4R-tau expression.

Seizure Severity Is Increased with 3R to 4R Splicing Change in hTau Mice

Emerging evidence strongly suggests a role for tau in modulating synaptic activity. Tau reduction, both genetically (Ittner et al., 2010; Roberson et al., 2007) and by ASO (DeVos et al., 2013), reduced seizure severity following pentylenetetrazole (PTZ) injection. At 4 months, hTau mice were treated with saline, scrambled ASO, or 3R to 4R splicing ASO infusion (n = 18–19/treatment) and, 1 month later, injected with PTZ to evoke a generalized seizure. Saline and scrambled ASO-treated mice were not statistically significant (mean seizure stage 3.64 ± 2.29 versus 4.00 ± 2.70 SD, respectively) and, therefore, combined for analyses. Compared to control treatments, 3R to 4R splicing ASO-treated hTau mice experienced significantly more severe seizures (p < 0.05; Figure 3A) and reached more severe

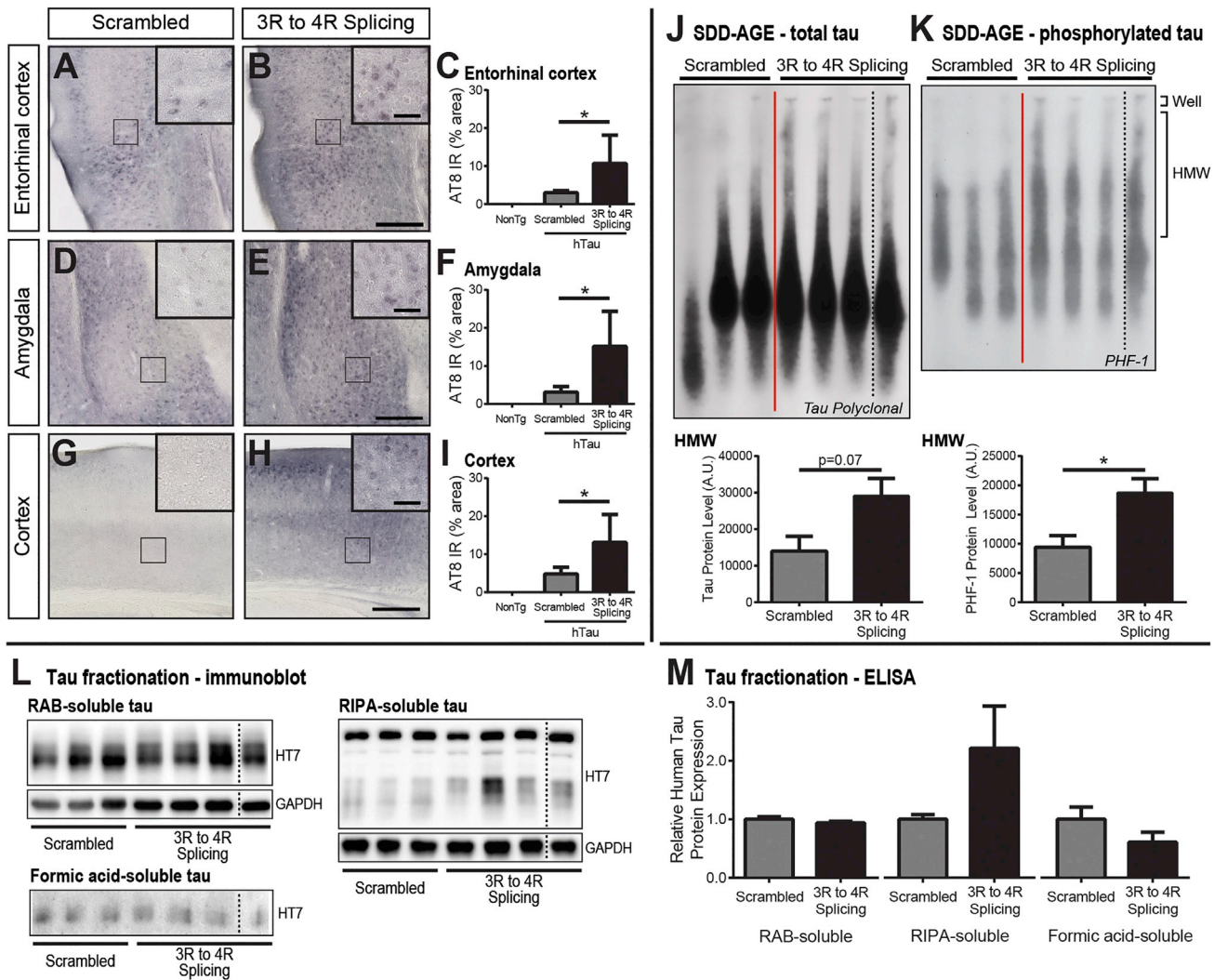


Figure 2. Detection of Phosphorylated and Aggregated Tau Species in ASO-Treated hTau Mice.

(A–I) Phosphorylated tau (AT8) was identified within the contralateral (A) entorhinal cortex, (D) amygdala, and (G) cortex of 4- and 12-month-old hTau mice following scrambled ASO treatment. Following 3R to 4R *MAPT* mRNA splicing ASO administration, AT8 cellular reactivity in these regions showed definitive increases (B, E, and H). Nontransgenic (NonTg) mice displayed no AT8 pathology. Of note, one mouse treated with 3R to 4R splicing ASO did not meet our established criteria for ASO treatment (i.e., 80% increase in 4R-tau mRNA) and was eliminated from pathological analysis. Scale bars represent 250 μ m, insets 50 μ m. The percentage of AT8 immunoreactivity (IR) within a given area was quantified by densitometric analysis, revealing greater AT8 IR with 3R to 4R splicing ASO treatment ($n = 7$) compared to NonTg ($n = 3$) or scrambled ASO ($n = 5$) treatment (C, F, and I); mean + SEM; * $p < 0.05$ scrambled versus splicing treatment. (J) Separation of monomeric tau from higher-order tau species by semidenaturing detergent agarose gel electrophoresis (SDD-AGE) revealed a shift toward more high-molecular-weight (HMW) tau forms with 3R to 4R splicing ASO treatment ($n = 4$) compared to scrambled control ($n = 3$) treatment in ipsilateral lysates obtained from 12-month-old hTau mice. When quantified by densitometric analysis, greater presence of HMW tau was identified with increased 4R-tau. (K) Tau was also significantly more heavily phosphorylated (PHF-1) with a 3R to 4R splicing change. (L) Ipsilateral cortical samples from treated hTau mice were fractionated and probed for human tau (HT7) to discern soluble versus insoluble tau forms. Increased 4R-tau expression appeared to shift human tau from the RAB-soluble fraction toward the RIPA-soluble fraction ($n = 3$ scrambled control, $n = 4$ 3R to 4R splicing ASO). No overt changes in insoluble tau in the formic acid fraction were detected between treatments. (M) Quantification of RAB-, RIPA-, and formic acid-soluble tau fractions by human-specific ELISA was comparable to immunoblot findings, demonstrating a modest increase in RIPA-soluble tau following 3R to 4R splicing ASO treatment. Data are expressed as mean + SEM; * $p < 0.05$. One lane of blots (black dashed lines) was cropped out to exclude the eliminated hTau sample within the 3R to 4R splicing ASO group.

seizure stages faster than controls ($p < 0.05$; Figure 3B). Despite the absence of overt synaptic or neuronal changes (Figure S3), these data strongly suggest that increasing 4R-tau worsens functional outcome in mice by either predisposing mice to seizure activity or exacerbating hyperexcitability.

Nesting Activity Is Impaired in hTau Mice with 3R to 4R *MAPT* Splicing

The natural behavior of nest building in mice has been used to assess impairment with AD and tauopathy (Torres-Lista and Giménez-Llort, 2013; Maeda et al., 2016) and can be quantified

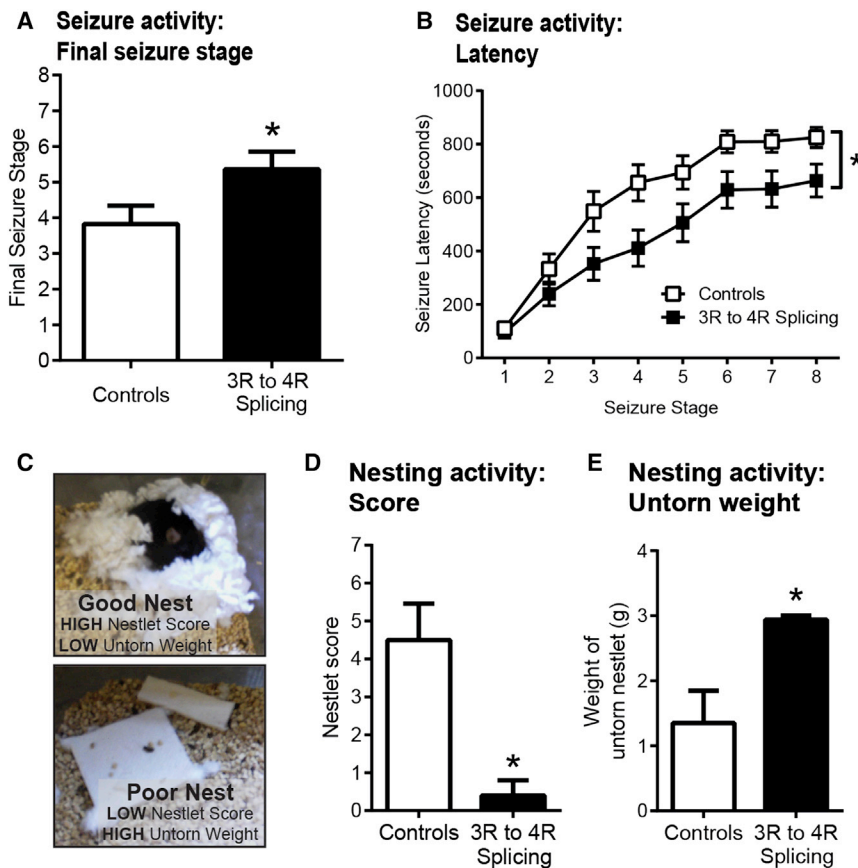


Figure 3. Functional Deficits Measured by Seizure and Nesting Activity in 3R to 4R MAPT mRNA Splicing ASO-Treated hTau Mice

(A and B) (A) Following intraperitoneal PTZ injection, hTau mice treated with 3R to 4R MAPT mRNA splicing ASO exhibited a significant increase in seizure severity and (B) a reduction in seizure latency compared to mice treated with saline or scrambled ASO (combined as controls) ($n = 18\text{--}19/\text{treatment}$). Final seizure score data are plotted as mean stage + SEM and seizure latencies are mean time \pm SEM across each seizure stage; * $p < 0.05$ versus controls.

(C–E) (C) Representative images of nests constructed by hTau mice. Nesting activity was assessed using a modified scoring criteria to rate the quality of nest construction and amount of torn nestlet material. hTau mice treated with 3R to 4R splicing ASO ($n = 5$) exhibited (D) significantly lower nestlet scores and (E) significantly greater untorn nestlet weights indicative of poor nesting activity compared to control (saline and scrambled ASO) treated hTau mice ($n = 5$). Nestlet scores and weights are shown as mean + SEM; * $p < 0.05$ versus controls.

based on published criteria (Figure 3A). Compared to male hTau mice treated with either saline or scrambled ASO ($n = 4$), hTau mice given 3R to 4R splicing ASO ($n = 5$) exhibited significantly lower nestlet scores ($p < 0.05$; Figure 3B) and greater weights of untorn nestlet ($p < 0.05$; Figure 3C), implicating increased 4R-tau in impaired nesting ability.

MAPT mRNA Splicing Alteration from 4R to 3R Is Effective in Human Tau-Expressing Mice

Our data and others' suggest 4R-tau to be more toxic, yet, to date, no tau splicing strategy has been implemented in vivo despite the overwhelming number of tau mutations within exon 10. In order to validate the use of an exon-skipping strategy in humans, we developed ASOs designed to exclude exon 10, thus decreasing 4R-tau without change to total tau levels, to test in hTau mice. Compared to saline treatment ($n = 3$), hTau mice that received 4R to 3R splicing ASO ($n = 3$) exhibited a robust decrease in exon 10 inclusion within the cortex ($p < 0.005$), hippocampus ($p < 0.05$), and spinal cord ($p < 0.005$; Figure 4A). Total tau levels remained unchanged (Figure 4B). To further address the efficacy and feasibility of a 4R to 3R splicing strategy, we applied this exon 10-skipping strategy to mice that recapitulate FTDP-17 tauopathy with mutant (TauN279K) 4R-tau overexpression (Dawson et al., 2007). Intraventricular administration of 4R to 3R splicing ASO resulted in a substantial decrease in 4R human MAPT mRNA concomitant with an increase in 3R MAPT mRNA

full-length human tau-expressing mice, lending support for the feasibility of a 4R isoform target in human dementias.

DISCUSSION

In hTau mice treated with ASO to increase 4R-tau, we identified a significant increase in phosphorylated tau and more-aggregated, less-soluble tau species. Seizures both were more severe and occurred at earlier time points with increased 4R-tau in hTau mice. While it is possible an imbalanced ratio of 4R-tau to 3R-tau or other off-target toxicity may have led to increased pathology, it remains likely that 4R-tau is more pathogenic. This is consistent with previous reports citing mitochondrial axonal transport defects (Stoothoff et al., 2009), microtubule instability (Bunker et al., 2004), and increased polymerization (Combs et al., 2011) of 4R-tau compared to 3R-tau. These altered characteristics may be key to the selective deposition of 4R-tau in progressive supranuclear palsy (PSP), corticobasal degeneration, and FTDP-17; however, other factors may influence the 3R-tau deposition seen in Pick's disease and the mixed deposition of both 3R-tau and 4R-tau in AD.

We also show in vivo application of the converse ASO approach by lowering 4R-tau in two mouse models of human tau expression. To date, nearly half of the 53 known MAPT mutations are located within exon/intron 10 (Ghetti et al., 2015) and account for 70% of the total number of published families

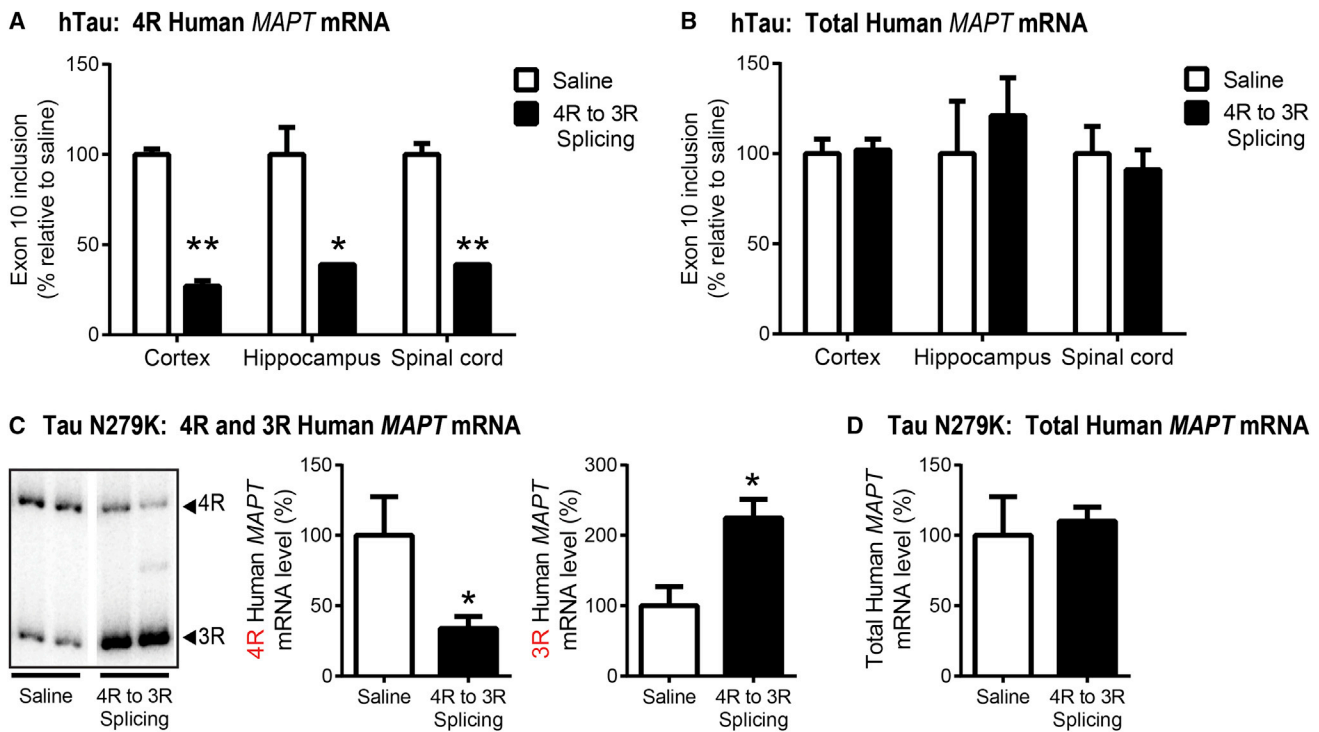


Figure 4. Validation of 4R to 3R Human MAPT mRNA Splicing ASOs In Vivo

In both hTau and Tau N279K mice, a reverse *MAPT* splicing strategy was investigated that would induce exon 10 skipping and bias toward 3R-tau. (A) In hTau mice, which exhibit tau isoform expression similar to humans, 4R to 3R *MAPT* splicing ASO induced a significant and widespread reduction of 4R mRNA levels in the cortex, hippocampus, and spinal cord compared to saline ($n = 3/\text{treatment}$). (B) No change in total tau mRNA was detected with either treatment. To further assess the potency of exon 10 exclusion, 4R to 3R splicing ASO was administered to Tau N279K mice and the ipsilateral temporoparietal cortex analyzed for *MAPT* isoform mRNA. (C and D) (C) Radiolabeled 4R and 3R PCR products demonstrate a clear shift toward 3R *MAPT* expression in mice treated with 4R to 3R splicing ASO ($n = 3$ saline, $n = 5$ ASO). When quantified, mRNA levels revealed that treatment with 4R to 3R splicing ASO afforded a significant decrease in 4R *MAPT* mRNA level and increase in 3R mRNA, in contrast to saline treatment, while (D) total human *MAPT* mRNA levels remained unchanged. 4R mRNA levels were calculated as a percent of exon 10 inclusion normalized to total tau, and total tau mRNA levels to GAPDH. Data are expressed as the percent of exon 10 inclusion relative to saline treatment (mean + SEM); analysis by unpaired t test (saline versus ASO) within each region, * $p < 0.05$, ** $p < 0.005$.

affected by *MAPT* mutations (Cruts et al., 2012). The 4R to 3R splicing ASO strategy described here would not only change 4R-tau to 3R-tau but would also remove the exon 10-containing amino acid missense mutation in the mature protein, without changing the total levels of tau. For PSP and other 4R-tauopathies without a primary tau mutation, exon 10 skipping may also be an advantageous therapy, since 4R-tau selectively deposits and is predicted to more readily seed 4R-tau (Dinkel et al., 2011; Sanders et al., 2014). Both exon 10-containing alleles would be targeted by our current ASO approach, although the concept of mutant allele-specific targeting has been successful in other models (Hu et al., 2009; Miller et al., 2003).

Overall, these data provide compelling evidence for the presence of tau isoform-mediated neurodegeneration and introduce exon 10-targeted ASOs that may be an effective therapy for tauopathies. A similar ASO-mediated exon skipping strategy has been successfully employed in Duchenne's muscular dystrophy (DMD). Exon skipping of a nonsense mutation restored dystrophin expression and improved motor function in mdx dystrophic mouse (Lu et al., 2003), leading to a dystrophin-targeting ASO (drisapersen) clinical trial in human DMD patients

(GlaxoSmithKline, 2014). The bench-to-bedside success of exon skipping in DMD in addition to the excellent safety profile of centrally delivered ASO for amyotrophic lateral sclerosis (Miller et al., 2013) and spinal muscular atrophy (Ionis Pharmaceuticals, 2016) emphasizes the promise of other ASO-mediated splicing strategies for the treatment of degenerative diseases. Alternative tau-targeted approaches, including tau clearance and total tau reduction, show promise for therapeutic applications but do not address the individual effect of tau isoforms in mediating tauopathies. And, in contrast to a total tau reduction approach, a *MAPT* splicing strategy would not affect total tau levels, thereby avoiding potential subtle or unforeseen confounds associated with a loss of tau (Lei et al., 2012; Ma et al., 2014; Dawson et al., 2010). In order to advance *MAPT* splicing ASOs toward human clinical trials, additional information will be necessary, including evaluation in preclinical tauopathy models, greater understanding of the 3R and 4R mRNA and protein composition in human tauopathies, and insight on what causes selective 4R deposition. Our experiments provide initial support for an ASO therapeutic strategy in primary tau mutations and potentially other 4R tauopathies.

EXPERIMENTAL PROCEDURES

Experimental Animals

Male and female hTau transgenic (Andorfer et al., 2003; RRID: IMSR_JAX: 005491) or tau N279K transgenic mice (Dawson et al., 2007) and their non-transgenic littermates were aged to 3–4 months prior to experimental treatment with the exception of biochemical and phosphorylated tau analyses in hTau mice (4 or 12 months of age). Ages/genders were matched across treatment groups. All husbandry and surgical procedures were approved by the Washington University Animal Studies Committee in accordance with federal standards. For more details on the animals used, refer to [Supplemental Information](#).

Antisense Oligonucleotides

Splicing ASOs were designed with a phosphorothioate backbone, uniformly modified with 2'-O-methoxyethyl nucleotides to enhance binding to the *MAPT* target and prevent RNaseH-mediated degradation of *MAPT* mRNA (DeVos and Miller, 2013a). A scrambled ASO control, designed with the same modifications as the *MAPT* splicing ASO but without target specificity, was included in experimental treatments to account for any potential toxicity or off-target effects of the ASO backbone. All ASOs were synthesized by Ionis Pharmaceuticals (Carlsbad, CA) and generously provided for use. ASO sequence information can be found in [Supplemental Information](#).

Intraventricular Delivery of ASOs

ASOs were continuously administered to the right lateral ventricle via osmotic pump (ALZET, Cupertino, CA) as previously described (DeVos and Miller, 2013b). For a detailed surgical procedure and osmotic pump preparation, see [Supplemental Information](#).

Euthanasia and Tissue Dissection

Mice were euthanized by transcardial perfusion with cold heparinized phosphate buffered saline (PBS) and decapitated. The right brain, ipsilateral to the catheter placement, was microdissected into temporoparietal and occipital regions (~15–30 mg), snap frozen in liquid nitrogen, and stored at –80°C until processing. The left brain was drop fixed into 4% paraformaldehyde for 24 hr followed by dehydration in 30% sucrose. Tissue was then frozen in –35°C to –25°C methylbutanes and stored at –80°C until sectioning for histology.

mRNA Isolation and Analysis

mRNA was isolated from temporoparietal right hemi-brain tissue. Total and *MAPT* isoform mRNA from hTau mice was readily detectable by standard quantitative real-time PCR methods. A modified RT-PCR protocol was used to amplify and detect human 3R and 4R *MAPT* isoforms in Tau N279K mice. Detailed methodology, including primer and probe sequences, is included under [Supplemental Information](#).

Tissue Homogenization and Tau Protein Analyses by ELISA and Immunoblot

Right hemibrain tissue designated for protein analysis was homogenized and prepared for analysis by ELISA and immunoblot as described in [Supplemental Information](#).

Detection of Tau by SDD-AGE

Semi-denaturing detergent agarose gel electrophoresis (SDD-AGE) was carried out as previously described (Sanders et al., 2014, Halfmann and Lindquist, 2008) with minor modifications (see [Supplemental Information](#)).

Immunohistochemistry of Phosphorylated Tau

Left hemibrain tissue from treated hTau mice was used for immunohistochemical detection of phosphorylated tau. Procedures, antibody information, and analyses are detailed in [Supplemental Information](#).

Seizure Induction and Monitoring

Seizure activity was induced by intraperitoneal injection of the GABA receptor antagonist, pentylenetetrazole (PTZ, Sigma), at a dose of 55 mg/kg and

analyzed as previously published (DeVos et al., 2013) and further described in [Supplemental Information](#).

Nesting Activity

Following the nocturnal period, untorn nesting material was weighed, and nests were photographed for scoring on a 0–7 ordinal scale modified from published criteria (Deacon, 2006, Gheyara et al., 2014) to assess both the percentage of chewed nestlet and shape of the nest. Additional detail has been provided in [Supplemental Information](#).

Statistics

Data were graphed as mean ± SEM and analyzed using GraphPad Prism 6 statistical software (GraphPad Software, La Jolla, CA). Individual statistical tests are described within [Supplemental Information](#).

SUPPLEMENTAL INFORMATION

Supplemental Information includes four figures and Supplemental Experimental Procedures and can be found with this article at <http://dx.doi.org/10.1016/j.neuron.2016.04.042>.

AUTHOR CONTRIBUTIONS

Conceptualization, K.M.S., S.L.D., C.F.B., F.R., and T.M.M.; Methodology, K.M.S., S.L.D., D.F.W., H.N.D., C.F.B., F.R., and T.M.M.; Investigation, K.M.S., S.L.D., R.L.M., S.J.C., and M.N.; Formal Analysis, K.M.S., S.L.D., D.F.W., F.R., and T.M.M.; Writing – Original Draft, K.M.S., S.L.D. and T.M.M.; Writing – Review & Editing, K.M.S., S.L.D., R.L.M., D.F.W., H.N.D., C.F.B., F.R., and T.M.M.; Funding acquisition, K.M.S. and T.M.M.; Supervision, C.F.B., F.R., and T.M.M.

ACKNOWLEDGMENTS

We wish to recognize and thank Dr. Bradley Hyman for the resources necessary to complete the biochemical tau experiments. We also thank the behavioral expertise provided by the Animal Behavior Core at Washington University in St. Louis, Dr. Peter Davies for his generous gift of the PHF-1 tau antibody, and Elena Fisher for her assistance in editing and preparing this manuscript. This work was supported by the Tau Consortium (T.M.M.), The National Institutes of Health (P50 AG05681 to T.M.M., J.C. Morris, PI; National Institute of Neurological Disorders and Stroke R01NS078398 to T.M.M. and F32 NS089225 to K.M.S.; and National Institute on Aging R21AG044719-01 to T.M.M.), Cure PSP (T.M.M.), and a Paul B. Beeson Career Development Award (NINDS K08NS074194 to T.M.M.). Microscopy was supported by the Hope Center Alafi Neuroimaging Laboratory and P30 Neuroscience Blueprint Interdisciplinary Center Core award to Washington University (P30 NS057105). Additional support was provided by the Gene Johnson Weston Brain Institute Advisor Fellowship to K.M.S. Antisense oligonucleotides used for experimental studies were generously provided by Ionis Pharmaceuticals. Washington University in St. Louis has filed patents in conjunction with Ionis Pharmaceuticals regarding use of Tau ASOs in neurodegenerative syndrome. S.J.C., M.N., C.F.B., and F.R. are paid employees of Ionis Pharmaceuticals.

Received: August 6, 2015

Revised: November 19, 2015

Accepted: April 26, 2016

Published: May 19, 2016

REFERENCES

- Adams, S.J., DeTure, M.A., McBride, M., Dickson, D.W., and Petrucelli, L. (2010). Three repeat isoforms of tau inhibit assembly of four repeat tau filaments. *PLoS ONE* 5, e10810.
- Andorfer, C., Kress, Y., Espinoza, M., de Silva, R., Tucker, K.L., Barde, Y.A., Duff, K., and Davies, P. (2003). Hyperphosphorylation and aggregation of tau in mice expressing normal human tau isoforms. *J. Neurochem.* 86, 582–590.

- Arai, T., Ikeda, K., Akiyama, H., Shikamoto, Y., Tsuchiya, K., Yagishita, S., Beach, T., Rogers, J., Schwab, C., and McGeer, P.L. (2001). Distinct isoforms of tau aggregated in neurons and glial cells in brains of patients with Pick's disease, corticobasal degeneration and progressive supranuclear palsy. *Acta Neuropathol.* *101*, 167–173.
- Braak, H., and Braak, E. (1995). Staging of Alzheimer's disease-related neurofibrillary changes. *Neurobiol. Aging* *16*, 271–278, discussion 278–284.
- Bunker, J.M., Wilson, L., Jordan, M.A., and Feinstein, S.C. (2004). Modulation of microtubule dynamics by tau in living cells: implications for development and neurodegeneration. *Mol. Biol. Cell* *15*, 2720–2728.
- Combs, B., Voss, K., and Gamblin, T.C. (2011). Pseudohyperphosphorylation has differential effects on polymerization and function of tau isoforms. *Biochemistry* *50*, 9446–9456.
- Cruts, M., Theuns, J., and Van Broeckhoven, C. (2012). Locus-specific mutation databases for neurodegenerative brain diseases. *Hum. Mutat.* *33*, 1340–1344.
- D'Souza, I., Poorkaj, P., Hong, M., Nochlin, D., Lee, V.M., Bird, T.D., and Schellenberg, G.D. (1999). Missense and silent tau gene mutations cause frontotemporal dementia with parkinsonism-chromosome 17 type, by affecting multiple alternative RNA splicing regulatory elements. *Proc. Natl. Acad. Sci. USA* *96*, 5598–5603.
- Dawson, H.N., Cantillana, V., Chen, L., and Vitek, M.P. (2007). The tau N279K exon 10 splicing mutation recapitulates frontotemporal dementia and parkinsonism linked to chromosome 17 tauopathy in a mouse model. *J. Neurosci.* *27*, 9155–9168.
- Dawson, H.N., Cantillana, V., Jansen, M., Wang, H., Vitek, M.P., Wilcock, D.M., Lynch, J.R., and Laskowitz, D.T. (2010). Loss of tau elicits axonal degeneration in a mouse model of Alzheimer's disease. *Neuroscience* *169*, 516–531.
- de Silva, R., Lashley, T., Gibb, G., Hanger, D., Hope, A., Reid, A., Bandopadhyay, R., Utton, M., Strand, C., Jowett, T., et al. (2003). Pathological inclusion bodies in tauopathies contain distinct complements of tau with three or four microtubule-binding repeat domains as demonstrated by new specific monoclonal antibodies. *Neuropathol. Appl. Neurobiol.* *29*, 288–302.
- Deacon, R.M. (2006). Assessing nest building in mice. *Nat. Protoc.* *1*, 1117–1119.
- DeVos, S.L., and Miller, T.M. (2013a). Antisense oligonucleotides: treating neurodegeneration at the level of RNA. *Neurotherapeutics* *10*, 486–497.
- DeVos, S.L., and Miller, T.M. (2013b). Direct intraventricular delivery of drugs to the rodent central nervous system. *J. Vis. Exp.* <http://dx.doi.org/10.3791/50326>.
- DeVos, S.L., Goncharoff, D.K., Chen, G., Kebodeaux, C.S., Yamada, K., Stewart, F.R., Schuler, D.R., Maloney, S.E., Wozniak, D.F., Rigo, F., et al. (2013). Antisense reduction of tau in adult mice protects against seizures. *J. Neurosci.* *33*, 12887–12897.
- Dinkel, P.D., Siddiqua, A., Huynh, H., Shah, M., and Margittai, M. (2011). Variations in filament conformation dictate seeding barrier between three- and four-repeat tau. *Biochemistry* *50*, 4330–4336.
- Ghetti, B., Oblak, A.L., Boeve, B.F., Johnson, K.A., Dickerson, B.C., and Goedert, M. (2015). Invited review: Frontotemporal dementia caused by microtubule-associated protein tau gene (MAPT) mutations: a chameleon for neuropathology and neuroimaging. *Neuropathol. Appl. Neurobiol.* *41*, 24–46.
- Gheyara, A.L., Ponnusamy, R., Djukic, B., Craft, R.J., Ho, K., Guo, W., Finucane, M.M., Sanchez, P.E., and Mucke, L. (2014). Tau reduction prevents disease in a mouse model of Dravet syndrome. *Ann. Neurol.* *76*, 443–456.
- GlaxoSmithKline (2014). Phase II Doubleblind Exploratory Study of GSK2402968 in Ambulant Subjects With Duchenne Muscular Dystrophy [Online]. Published online August 21, 2014. <https://www.clinicaltrials.gov/ct2/show/NCT01153932>.
- Halfmann, R., and Lindquist, S. (2008). Screening for amyloid aggregation by semi-denaturing detergent-agarose gel electrophoresis. *J. Vis. Exp.* <http://dx.doi.org/10.3791/838>.
- Hong, M., Zhukareva, V., Vogelsberg-Ragaglia, V., Wszolek, Z., Reed, L., Miller, B.I., Geschwind, D.H., Bird, T.D., McKeel, D., Goate, A., et al. (1998). Mutation-specific functional impairments in distinct tau isoforms of hereditary FTDP-17. *Science* *282*, 1914–1917.
- Hu, J., Matsui, M., Gagnon, K.T., Schwartz, J.C., Gabillet, S., Arar, K., Wu, J., Bezprozvanny, I., and Corey, D.R. (2009). Allele-specific silencing of mutant huntingtin and ataxin-3 genes by targeting expanded CAG repeats in mRNAs. *Nat. Biotechnol.* *27*, 478–484.
- Ionis Pharmaceuticals (2016). A Study to Assess the Efficacy and Safety of ISIS-SMN Rx in Infants With Spinal Muscular Atrophy [Online]. Published online May 6, 2016. Available: <https://clinicaltrials.gov/ct2/show/NCT02193074>.
- Ittner, L.M., Ke, Y.D., Delerue, F., Bi, M., Gladbach, A., van Eersel, J., Wöfling, H., Chieng, B.C., Christie, M.J., Napier, I.A., et al. (2010). Dendritic function of tau mediates amyloid-beta toxicity in Alzheimer's disease mouse models. *Cell* *142*, 387–397.
- Lei, P., Ayton, S., Finkelstein, D.I., Spoorri, L., Ciccotosto, G.D., Wright, D.K., Wong, B.X., Adlard, P.A., Cherny, R.A., Lam, L.Q., et al. (2012). Tau deficiency induces parkinsonism with dementia by impairing APP-mediated iron export. *Nat. Med.* *18*, 291–295.
- Lu, Q.L., Mann, C.J., Lou, F., Bou-Gharios, G., Morris, G.E., Xue, S.A., Fletcher, S., Partridge, T.A., and Wilton, S.D. (2003). Functional amounts of dystrophin produced by skipping the mutated exon in the mdx dystrophic mouse. *Nat. Med.* *9*, 1009–1014.
- Ma, Q.L., Zuo, X., Yang, F., Ubeda, O.J., Gant, D.J., Alaverdyan, M., Kiosea, N.C., Nazari, S., Chen, P.P., Nothias, F., et al. (2014). Loss of MAP function leads to hippocampal synapse loss and deficits in the Morris Water Maze with aging. *J. Neurosci.* *34*, 7124–7136.
- Maeda, S., Djukic, B., Taneja, P., Yu, G.Q., Lo, I., Davis, A., Craft, R., Guo, W., Wang, X., Kim, D., et al. (2016). Expression of A152T human tau causes age-dependent neuronal dysfunction and loss in transgenic mice. *EMBO Rep.* *17*, 530–551.
- Miller, V.M., Xia, H., Marrs, G.L., Gouvion, C.M., Lee, G., Davidson, B.L., and Paulson, H.L. (2003). Allele-specific silencing of dominant disease genes. *Proc. Natl. Acad. Sci. USA* *100*, 7195–7200.
- Miller, T.M., Pestronk, A., David, W., Rothstein, J., Simpson, E., Appel, S.H., Andres, P.L., Mahoney, K., Allred, P., Alexander, K., et al. (2013). An antisense oligonucleotide against SOD1 delivered intrathecally for patients with SOD1 familial amyotrophic lateral sclerosis: a phase 1, randomised, first-in-man study. *Lancet Neurol.* *12*, 435–442.
- Polydoro, M., Acker, C.M., Duff, K., Castillo, P.E., and Davies, P. (2009). Age-dependent impairment of cognitive and synaptic function in the htau mouse model of tau pathology. *J. Neurosci.* *29*, 10741–10749.
- Roberson, E.D., Searce-Levie, K., Palop, J.J., Yan, F., Cheng, I.H., Wu, T., Gerstein, H., Yu, G.Q., and Mucke, L. (2007). Reducing endogenous tau ameliorates amyloid beta-induced deficits in an Alzheimer's disease mouse model. *Science* *316*, 750–754.
- Sanders, D.W., Kaufman, S.K., DeVos, S.L., Sharma, A.M., Mirbaha, H., Li, A., Barker, S.J., Foley, A.C., Thorpe, J.R., Serpell, L.C., et al. (2014). Distinct tau prion strains propagate in cells and mice and define different tauopathies. *Neuron* *82*, 1271–1288.
- Spillantini, M.G., and Goedert, M. (2013). Tau pathology and neurodegeneration. *Lancet Neurol.* *12*, 609–622.
- Stoothoff, W., Jones, P.B., Spires-Jones, T.L., Joyner, D., Chhabra, E., Bercury, K., Fan, Z., Xie, H., Bacskai, B., Edd, J., et al. (2009). Differential effect of three-repeat and four-repeat tau on mitochondrial axonal transport. *J. Neurochem.* *111*, 417–427.
- Torres-Lista, V., and Giménez-Llort, L. (2013). Impairment of nesting behaviour in 3xTg-AD mice. *Behav. Brain Res.* *247*, 153–157.
- von Bergen, M., Barghorn, S., Li, L., Marx, A., Biernat, J., Mandelkow, E.M., and Mandelkow, E. (2001). Mutations of tau protein in frontotemporal dementia promote aggregation of paired helical filaments by enhancing local beta-structure. *J. Biol. Chem.* *276*, 48165–48174.